Sauter, Caspar; Grether, Jean-Marie; Mathys, Nicole A.

Working Paper

Back to 1820? Spatial distribution of GDP and CO2 Emissions

IRENE Working Paper, No. 15-05

Provided in Cooperation with:
Institute of Economic Research (IRENE), University of Neuchâtel

Suggested Citation: Sauter, Caspar; Grether, Jean-Marie; Mathys, Nicole A. (2015) : Back to 1820? Spatial distribution of GDP and CO2 Emissions, IRENE Working Paper, No. 15-05, University of Neuchâtel, Institute of Economic Research (IRENE), Neuchâtel

This Version is available at:
https://hdl.handle.net/10419/191476

University of Neuchatel

Institute of Economic Research

IRENE, Working paper 15-05

Back to 1820?

Spatial distribution of GDP and CO_2 Emissions

Caspar Sauter, Jean-Marie Grether* and Nicole A. Mathys***

** University of Neuchatel, Faculty of Economics and Business*

***Federal Office for Spatial Development, Berne and*
University of Neuchatel, Faculty of Economics and Business

UNIVERSITÉ DE NEUCHÂTEL

Institut de recherches économiques

Back to 1820? Spatial distribution of GDP and CO_2 Emissions

May 2015

Caspar Sauter[a], Jean-Marie Grether[a,*], Nicole Mathys[b,a]

[a] *University of Neuchatel, Faculty of Economics and Business*
[b] *Federal Office for Spatial Development, Berne*

Abstract

We construct the world's centers of gravity for human population, GDP and CO_2 emissions by taking the best out of five recognized data sources covering the last two centuries. We also propose a more appropriate two-map representation of the location of the center of gravity, which abstracts from the usual distortions affecting the projection of a point within a three-dimensional sphere on a two-dimensional map. This allows for a more accurate interpretation of the underlying trends. We find a radical Western shift of GDP and CO_2 emissions centers during the 19th century, in sharp contrast with the stability of the demographic center of gravity. Both GDP and emissions trends are reversed in the first half of the 20th century, after World War I for CO_2 emissions, and after World War II for GDP. Since then, both centers are moving eastward at an accelerating speed. These patterns are consistent with the initial lead of Western countries starting the industrial revolution and the adoption of fossil fuels as its main energy source, the impact of world conflicts, the gradual replacement of coal by oil and gas, and the progressive catch up of Asian countries, leading to a convergence in terms of both GDP and CO_2 emissions per capita in the recent past.

Keywords: center of gravity, growth, CO_2 emissions, gdp, population, convergence

1. Introduction

A better understanding of global issues, such as Climate Change or the adoption of Sustainable Development Goals, requires indicators that are both global in scope and synthetic in nature. In this paper, we propose to revisit the concept of the world center of gravity, which collapses into a single point the distribution of any variable upon the Earth's surface. This allows to identify non-trivial trends and structural shifts at the global level. To illustrate the relevance of this indicator, we apply it to an original combination of historical data sources, in order to compare the evolution of both GDP and CO_2 emissions on the Earth's surface since 1820.

The first applications of the center of gravity, by Grether and Mathys (2010) and Quah (2011), were limited to global production and recent decades. Although using different projection methods

☆JEL classification: Q56, Q59
*Corresponding author
Email addresses: caspar.sauter@unine.ch (Caspar Sauter), jean-marie.grether@unine.ch (Jean-Marie Grether), nicole.mathys@gmail.com (Nicole Mathys)

to represent the center of gravity, they relied on the same database for GDP (World Bank indicators) and its approximate within-country spread (using city population data), and confirmed a clear Eastern shift since 1980. These early applications toppled with two major problems namely how to spread more accurately GDP within countries and how to go further backward in time. These issues were addressed in two subsequent papers.

Instead of using cities, Grether and Mathys (2011) rely on gridded data provided by the G-Econ database (Nordhaus et al., 2006), which provide a more accurate measure of the spatial distribution of population and production. They also use the Maddison (2010) database for older values of GDP but stop in 1950 due to missing data prior to that year. This later obstacle is lifted by **?** who provide a thorough discussion of the original Maddison database and the additional assumptions that are necessary to extend it before 1950. Although pre-industrial data must be taken with a grain of salt, their results are clearly suggestive of a strong Western shift along with the Big Divergence, with a trend reversal in 1920 for the demographic center, and in 1950 for the economic center. This suggests that the former debate of the sixties, whether the unprecedented growth that followed the industrial revolution in Western countries could also be experienced by other countries as well (e.g. Bairoch (1971)), could have been clarified much earlier if better data and more accurate indicators had been made available.

One important drawback of these last two historical papers is that, for all years for which gridded data are still not available, the assumption is simply that grid shares at the country level are kept unchanged with respect to the closest available year (i.e. 1990 for G-Econ). This is of particular concern for countries like the US or China, which cover large areas, represent a significant share of world totals, and where the distribution of people and economic activity has suffered structural changes over the last two centuries. The present paper offers a welcome improvement with respect to that shortcoming, by exploiting the Hyde 3.1 database (Klein Goldewijk et al., 2011), which provides gridded population data at a very disaggregated level. This database goes back as far as 1750, and has already been exploited by long run studies of land-use by human populations (Ellis et al., 2013) and its relationship with global warming (Matthews et al., 2014). This allows to spread national totals regarding GDP (or CO_2 emissions) according to varying population shares back in the past rather than by applying fixed shares.

Apart from this unprecedented accuracy, the present paper extends the literature in two other directions. First, it adds an environmental dimension to the analysis, namely CO_2 emissions, relying on gridded data provided by the EDGAR database since 1970, and on the CDIAC database for earlier years. This allows to compare the distribution of both economic activity and the major source of greenhouse gases since the first stages of the industrial revolution. As such, it provides a concise description of the dynamics of world imbalances during the last two centuries, illustrating the historic responsibility of the West, which is a cornerstone of present negotiations to tackle Climate Change (e.g. Barrett and Stavins (2003) or Mattoo and Subramanian (2012)). It turns out that the emission center of gravity mimics the Western shift of the economic center during the 19th century, but shifts back towards Asia thirty years earlier, at the beginning of the 20th century.

Finally, we provide a thorough discussion on how best to represent a world center of gravity onto a map. This is not evident, as the usual distortions of distances by latitude and longitude are compounded by the fact that the center of gravity locates underground, not on the Earth's surface.

We propose here an original two-map approach, which is both visually telling and distortion-free in representing the Cartesian coordinates of the center of gravity. This is important as the alternative projection methods used until now tend to magnify errors in measurement when the center of gravity is close to the center of the Earth, which happens to be the case in recent decades.

2. Methodology

2.1. Cartesian coordinates of world centers of gravity

Assume the surface of the Earth is covered by a regular grid of N cells. Each cell i, $i = 1, ..., N$, is identified by the latitude (φ) and longitude (λ) of its lower-left corner. For each cell, there is an estimate of the underlying variable V, i.e. CO_2 emissions (E) for the world emission center of gravity, GDP (G) for the world economic center of gravity, or population (P) for the world demographic center of gravity.

The Cartesian coordinates of each center of gravity are determined according to the three-step methodology previously introduced by Grether and Mathys (2010). First, the share of each cell in the world total is calculated, i.e. $s_{iV} = \frac{V_i}{\sum_{i=1}^{N} V_i}$. Second, the Polar coordinates of each grid cell are converted into their corresponding Cartesian coordinates, denoted by x, y and z. For that purpose, the Earth is assumed to be a perfect sphere, a reasonable assumption given the approximations affecting the measurement of the underlying variables. Cartesian coordinates may be expressed in kilometers, or as a fraction of the Earth's radius, R (6371km).[1] Third, the coordinates of the world center of gravity are obtained as weighted averages of the Cartesian coordinates of each grid cell, using grid cell shares as weights:

$$x_v = \sum_{i=1}^{N} s_{iV} x_i \qquad y_v = \sum_{i=1}^{N} s_{iV} y_i, \qquad z_V = \sum_{i=1}^{N} s_{iV} z_i \tag{1}$$

The obtained point, $P_V^*(x_V, y_V, z_V)$, where $V = E, G, P$, locates within the sphere. The length of the associated vector, with its origin in the Earth's center, is obtained as:

$$\left\| \overrightarrow{OP_V^*} \right\| = \sqrt{x_V^2 + y_V^2 + z_V^2} \tag{2}$$

This length can be used as a rough indicator of the concentration of the underlying variable on the Earth's surface. An extreme concentration in a single point would lead to a gravity center right on the Earth's surface, and a length just equal to the Earth's radius.

2.2. Existing conventions to represent the location of world centers of gravity

The literature on how to map the Earth's surface on a two-dimensional plane dates back to more than two thousand years (see Snyder (1987) for a detailed survey including both technical and historical references). There is no universally accepted technique, as every method (cylindrical, conic or azimuthal, and their sub-cases) presents its shortcomings regarding specific distortions (e.g.

[1] In a 3-dimensional space where the origin is at the center of the Earth, axis x (projection of the Greenwich meridian) and y (projection of the 90°E meridian) define the equatorial plane, and axis z is the North-South polar axis, the corresponding formulas are : $x_i = Rcos(\varphi_i)cos(\lambda_i)$, $y_i = Rcos(\varphi_i)sin(\lambda_i)$, $z_i = Rsin(\varphi_i)$, where R is the Earth's radius. See the technical Appendix to Grether and Mathys (2011) for a detailed description.

on distances, areas or angles). The problem is further compounded here by the fact that the points we are interested in, i.e. the centers of gravity, are located *within* the sphere, not on its surface.

To the best of our knowledge, two projection techniques have been proposed till now for the world centers of gravity, as illustrated by Figure 1. The first one, proposed by Grether and Mathys (2010), consists of projecting orthogonally the center of gravity, P^*, upon the Earth's surface (Figure 1a). It leaves unspecified the technique used to represent the projection point, P_1, with latitude φ_1. The second technique, proposed by Quah (2011), directly projects the center of gravity on a cylinder wrapping the globe along the Equator (Figure 1b), which leads to a lower latitude for the projection point, $\varphi_2 < \varphi_1$.

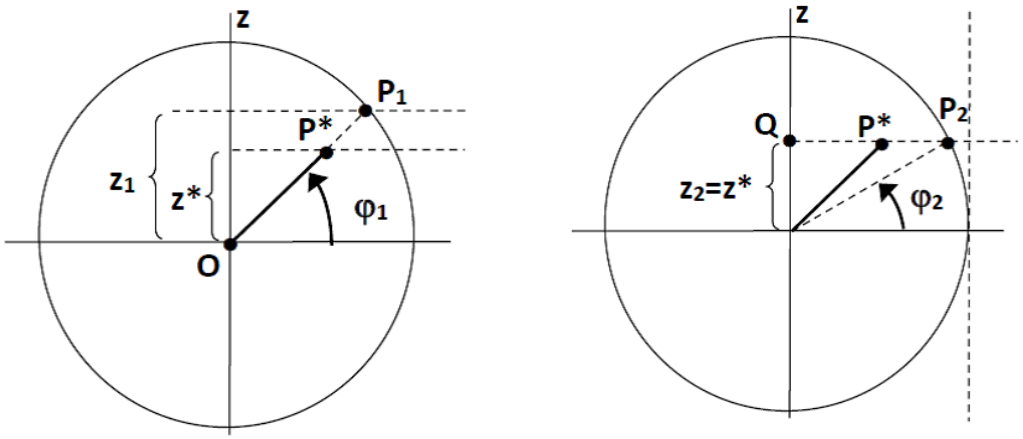

(a) Grether and Mathys (2010) (b) Quah (2011)

Figure 1: Alternative projections of the world's center of gravity

Both techniques may be criticized on the ground that they are insensitive to specific directional movements of the center of gravity, depending on the distribution of the underlying variable over time. The convention by Grether and Mathys (2011) does not capture changes of P^* along the OP_1 axis. The convention by Quah (2011) is insensitive to changes of P^* along the QP_2 line. Which type of changes matters more in practice is an empirical question, which could guide the choice between these two projection techniques, or any other alternative deemed more relevant depending on the specific variable or time period considered. However, any convention relying on a single two-dimensional map will remain affected by some kind of distortion. That is why we privilege here Cartesian over Geographic coordinates, and use two maps instead of a single one. We argue in the next subsection that this is the most accurate and tractable way to represent a point located deeply underground.

2.3. A new, distortion-free convention

The first map, on the left of Figure 2, is consistent with the technique of Quah (2011) that is, a cylindrical projection. It provides, on the vertical axis, a distortion-free representation of

the z Cartesian coordinate described in subsection 2.1. The horizontal axis represents longitude, which is subject to distortions, because there is an infinity of (x, y) combinations *within the sphere* corresponding to the same longitude. The second diagram on the right of Figure 2, provides an explicit representation of x and y, with the $x(y)$ axis representing the projection of the Greenwich (90 degree) meridian. All three Cartesian coordinates are expressed as a fraction of the Earth's radius.[2]

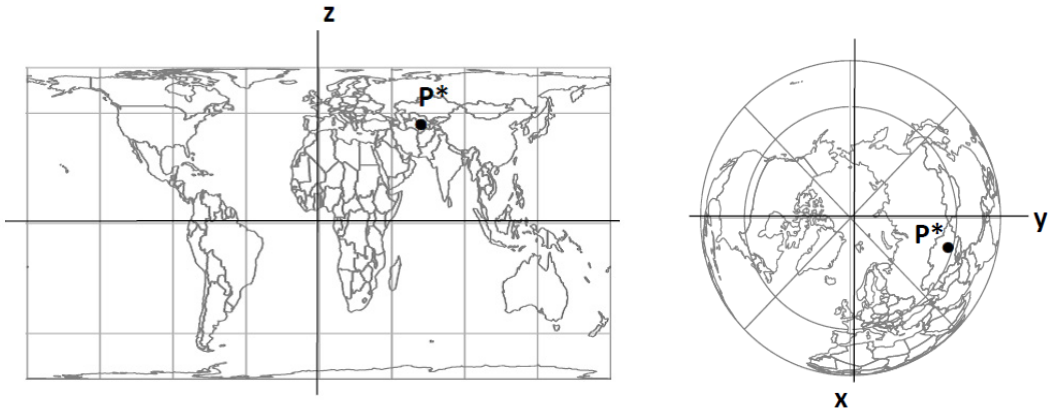

(a) cylindrical projection (b) azimuthal projection

Figure 2: Cartesian coordinates of the gravity center in two maps

The combination of these two maps allows describing without distortion any underground movement of the center of gravity, including those above-mentioned peculiar cases for which previously used conventions are insensitive to. Two stylized examples will help to illustrate the complementarity of both maps. In each case, one of the two maps gives a confusing vision of the evolution of the center of gravity, while the other map unveils what actually happens. We dub the first case the "wipper effect". It is represented in Figure 3, where the left map suggests that the center of gravity shifts from point A to point B, then back again, and so forth, as a pendulum covering apparently the same horizontal distance period after period. However, what happens in reality, as shown by the right map, is that the center of gravity gets ever closer to the center of the Earth, along a zigzag trajectory analogous to the one of a bug crawling from the extremity of a car wiper to its rotating base. Again, this illusion is due to the fact that an infinity of within-sphere (x, y) combinations are compatible with the same longitude.

The right map is not exempt from optical illusion either. In the second case, illustrated in Figure 4, the center of gravity appears to be going round a regular ellipse on the right map. However, the left map shows that its height above the equatorial plane is regularly decreasing. We call that movement along a downward spiral a "staircase" effect.

Other optical illusions could still be considered but are not reported here for the sake of con-

[2]Countries' contours correspond to a Lambert equal-area cylindrical projection in the left map, and to an azimuthal projection in the right map. Figures 2-4 limit the number of meridians and parallels to streamline presentation. Consecutive figures with actual results report meridians and parallels every 10°, along with ticks to indicate half of the Earth's radius on the x,y,z axis.

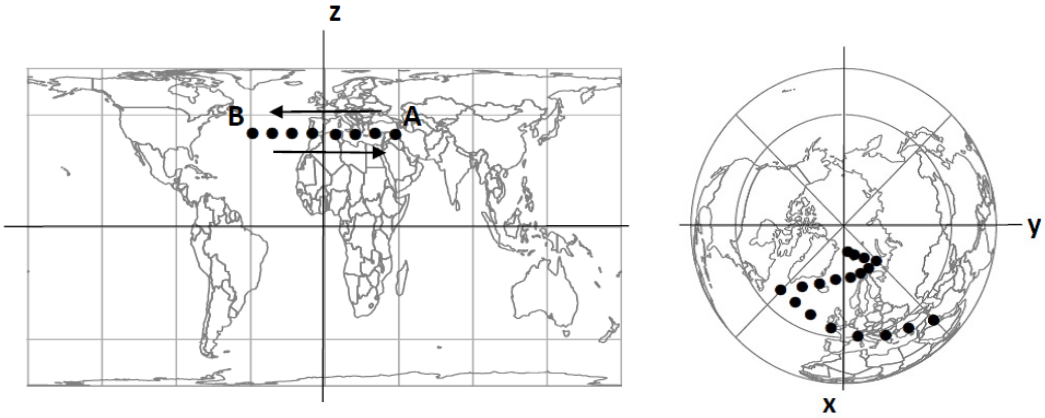

(a) (b)

Figure 3: The "wiper" effect

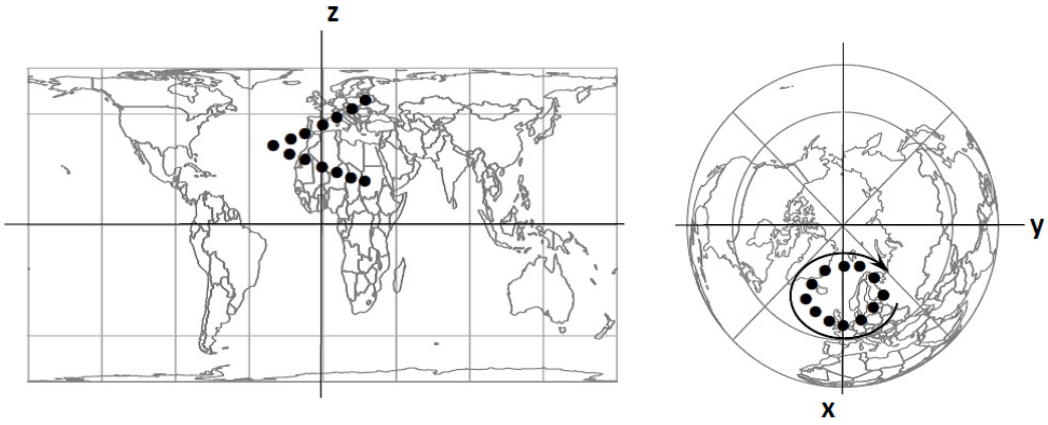

(a) (b)

Figure 4: The "staircase" effect

ciseness, and as we limit the presentation to the two cases which do affect our own results. The key point is that, although we keep on using latitudes and longitudes to characterize locations on maps, the center of gravity is an underground point which is best identified in space by using three Cartesian coordinates rather than two Geographic coordinates.

3. Data sources

Data needed for calculations are obtained by combining five distinct data sources. On the one hand, three data bases provide information at the grid level. The HYDE 3.1 database (Klein Gold-

ewijk et al., 2011) provides historical gridded population data from 10000 B.C to 2005 A.D. Since 1820, the data is available in 10 year intervals, and has a grid resolution of 5 by 5 arc minutes. The G-Econ research project (see G-Econ (2011)) provides gridded GDP data at a 60 arc minutes level of resolution for the years 1990, 1995, 2000 and 2005. The Emission Database for Global Atmospheric Research (EDGAR, see European Commission and Joint Research Centre (JRC)/Netherlands Environmental Assessment Agency (PBL) (2011)) reports yearly data on CO_2 emissions from fuel combustion and non-metallic mineral processes (including cement production)[3] , excluding short-cycle organic carbon from biomass burning at a 0.1° level of resolution. This data covers the period of 1970 to 2008. On the other hand, two other data bases cover larger periods but at the national level only, i.e. the The Maddison Project (2013), which contains estimates of GDP and population from 1 to 2010 A.D., and CDIAC (see Boden et al. (2013)), which provides CO_2 estimates from fossil-fuel consumption and cement production over the 1751-2010 period.

3.1. Population

The only modification of the HYDE database is to extend it from 2005 to 2010. To do so, we apply to each cell's population in 2005 the population growth rate 2005-2010 of the corresponding country as obtained from the national figures of the Maddison database. Country attribution of each cell is obtained by merging HYDE with the global database on administrative boundaries GADM (2012). As explained below, this HYDE gridded population database at a very high degree of resolution provides the basis to extend the GDP and emission gridded data backward in time.

3.2. GDP

First, the G-Econ 2005 gridded GDP data are extended to 2010, using Maddison country GDP data for growth rates and by relying on the same method as described above for population. Second, we extend the gridded GDP series backward to 1820 in the following way. We combine the HYDE and the Maddison databases by assuming that within-country GDP is uniformly distributed per capita. This allows to spread national GDP figures from the Maddison database according to the gridded population shares obtained from the HYDE database. The obtained Maddison/HYDE gridded GDP figures are of course an approximation, but given data availability, it is the best way to capture within-country spatial variations backward in time. We then aggregate the so obtained 5 arc minutes cells to cells with a 60 arc minutes resolution in order to match them with the G-Econ data. Finally, we merge the Maddison/HYDE data, covering the decades 1820 to 2000, with the G-Econ database, which covers the years 1990 to 2010.[4] Whenever possible, we construct 5 year averages around decimal years to minimize the influence of potential extreme events.

3.3. CO_2 emissions

The procedure is similar to the one followed for GDP. First, gridded EDGAR emission data for 2008 are extended to 2012 by using 2008-2010 and 2010-2012 national growth rates obtained

[3]Note that Edgar covers more carbon dioxide sources, but to correctly match Edgar with CDIAC (which covers only CO_2 emissions from fossil-fuel consumption and cement production), we retain from EDGAR only CO_2 emissions from IPCC source category 1A (fuel combustion) and 2A (non-metallic mineral processes).

[4]To avoid potential jumps in the final series, we smooth the transition from one database to the other by using a mix of both cell GDP datasets for overlapping decades 1990 and 2000. For the year 1990, we calculate final cell GDP as 70% of Maddison/HYDE cell GDP and 30% of G-Econ cell GDP, while for the year 2000 we calculate it as 30% Maddison/HYDE cell GDP and 70% G-Econ cell GDP.

from the EDGAR FT2012 database (an extended version of Edgar v4.2, containing country data). Second, to extend data backward in time, the HYDE and CDIAC databases are combined assuming emissions per capita are uniformly spread within countries. Then the obtained CDIAC/HYDE data are aggregated to a 60 arc minutes resolution to harmonize with the GDP aggregation level. Finally, we merge the CDIAC/HYDE data, covering the years 1820 to 1990 with the EDGAR database which covers the years 1970 to 2010.[5] Whenever possible, we construct 5 year averages around decimal years to minimize the influence of potential extreme events.

4. Results

Figures 5, 6 and 7 report the two-map diagrams for the three centers of gravity, i.e. for population, GDP and CO_2 emissions. We remind the reader that the country frontiers are only reported here for graphical convenience. Normally the center of gravity itself always locates well below the Earth's surface. Its height (coordinates along orthogonal meridians) above (within) the equatorial plane is (are) given in the left (right) map.

Figure 8a compares the length of the gravity vectors, as the distance between the gravity center and the Earth's center. It is a rough measure of the concentration of the underlying variable on the Earth's surface. It also helps figuring out the radius of the inner-Earth imaginary concentric sphere upon which the center of gravity locates. Figure 8b compares the speed of the gravity centers, i.e. the distance they cover per decade.

Regarding interpretation of trends, the coordinates of the world center of gravity being a weighted average of individual cell's coordinates, it is intuitive that changes over time are mostly driven by variations in (large) country shares.[6] To condense presentation, we will only refer to the most important changes in the text below. The interested reader can also refer to the Appendix for the evolution of the share of the largest countries during the 1820-2010 period.

4.1. Population

As could be expected, the population center of gravity is basically located under Asia (Northern India in the left maps and along the Russian-Kazak frontier in the right maps). At the beginning of the period, its length is close to 5000 km, i.e. around 0.75R, where R is the Earth's radius (6371 km). This is the result of 0.5R elevation over the equatorial plane (corresponding to a Northern latitude of 30°) and approximately 0.6R rightward orientation on the projection of the 90° meridian (the coordinate along the projection of the Greenwich meridian is almost negligible). In short, human population is initially quite concentrated in the Asian part of the Northern hemisphere.

The bottom maps reveal a small but steady shift during the sample period, in two distinct phases. During the first phase, which lasts until 1910, the center of gravity shifts westward, with no

[5] To avoid potential jumps in the final series, we smooth the transition from one database to the other by using a mix of both cell CO_2 datasets for the years 1970, 1980 and 1990, as we did for GDP. For 1970 (1980, 1990), we calculate final cell CO_2 emissions as 75% (50%, 25%) of CDIAC/HYDE cell emissions and 25% (50%, 75%) of EDGAR cell emissions.

[6] In theory, within-country variation should also be addressed, but in practice, most of the variation comes from between-country changes. See also **?** for a decomposition of changes of the economic center of gravity into between-continent and within-continent effects.

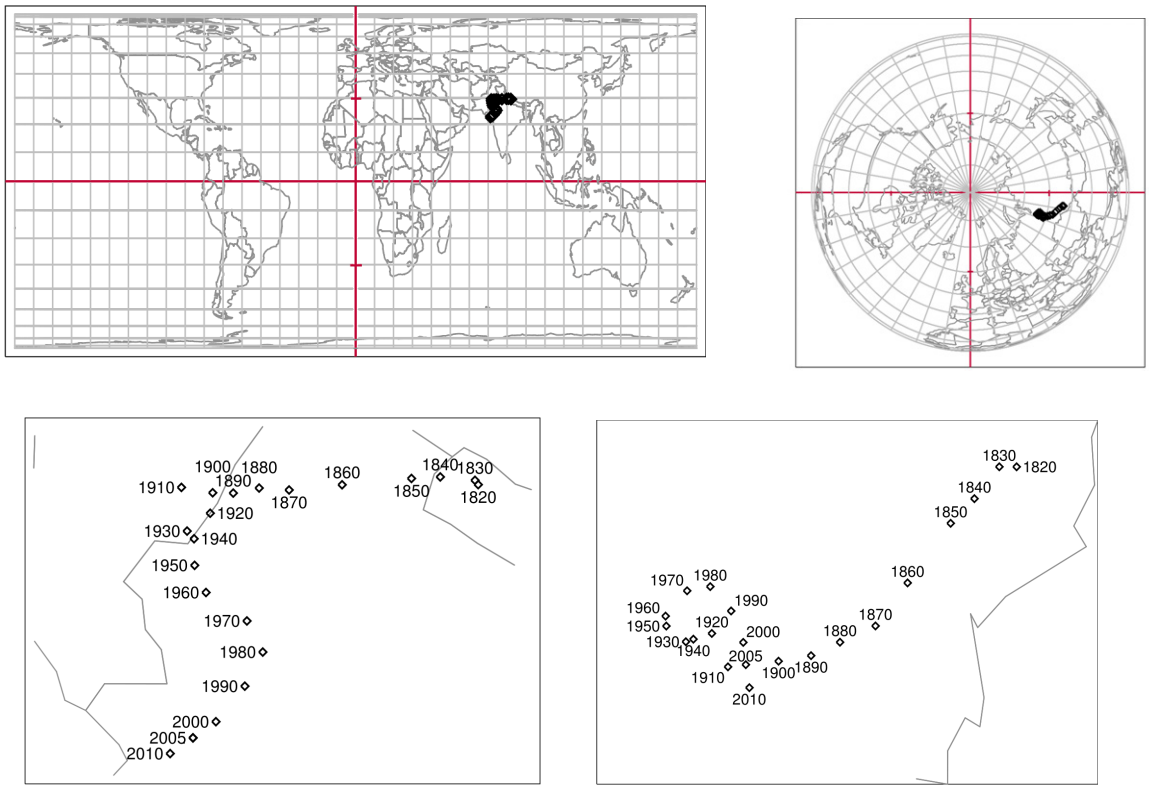

Figure 5: Center of gravity for population

latitudinal change. This is consistent with the gradual decline of China and India, whose combined share in world population drops from 55% to 40% along that sub-period. It is also concomitant with a leftward shift of the horizontal component of the left maps, and a corresponding decline in the length of the gravity vector by around 15%. That is, human population becomes more homogeneously spread, with a decline in Eastern and a rise in Western locations, in particular the USA.

During the second phase, starting in 1920, there is a clear Southern shift, slightly eastward until 1980, and westward since then. This is consistent with Western countries plateauing in terms of population, the combined share of China and India remaining roughly constant, and a relative increase of Southern countries in East Asia first, and in Africa second. Overall, there is again an increase in the dispersion of human population, although the decline of the length of the gravity vector is more moderate than in the first phase.

These shifts in the demographic gravity center are consistent with historical trends, but of modest magnitude, with an average speed of less than 200km per decade. The trends exhibited by the other two variables reveal more profound changes.

4.2. GDP

The trajectory of the economic center of gravity is also in two phases, but the striking features are that apparent distances covered are far larger than for the demographic center, whereas the elevation upon the equatorial plane is almost unchanged, with most points locating along the 30°N parallel on left-hand side maps. Starting 1820, the location is almost identical to the demographic center of gravity, reflecting the small differences in GDP per capita across countries prior to the industrial revolution. Then the Big Divergence leads to a strong western shift of the economic gravity center, with a speed two to three times larger than for the demographic center of gravity, and during a longer period. Although the 1930s and 1940s slow down the process, the immediate aftermaths of World War II brings it its last big western push, with a 1950 location close to the middle of the Atlantic. During that same sub-period, the combined share of China and India in world GDP has dropped from 45% to less than 10%, while that of the USA has risen from a few percentage points to more than 25%.

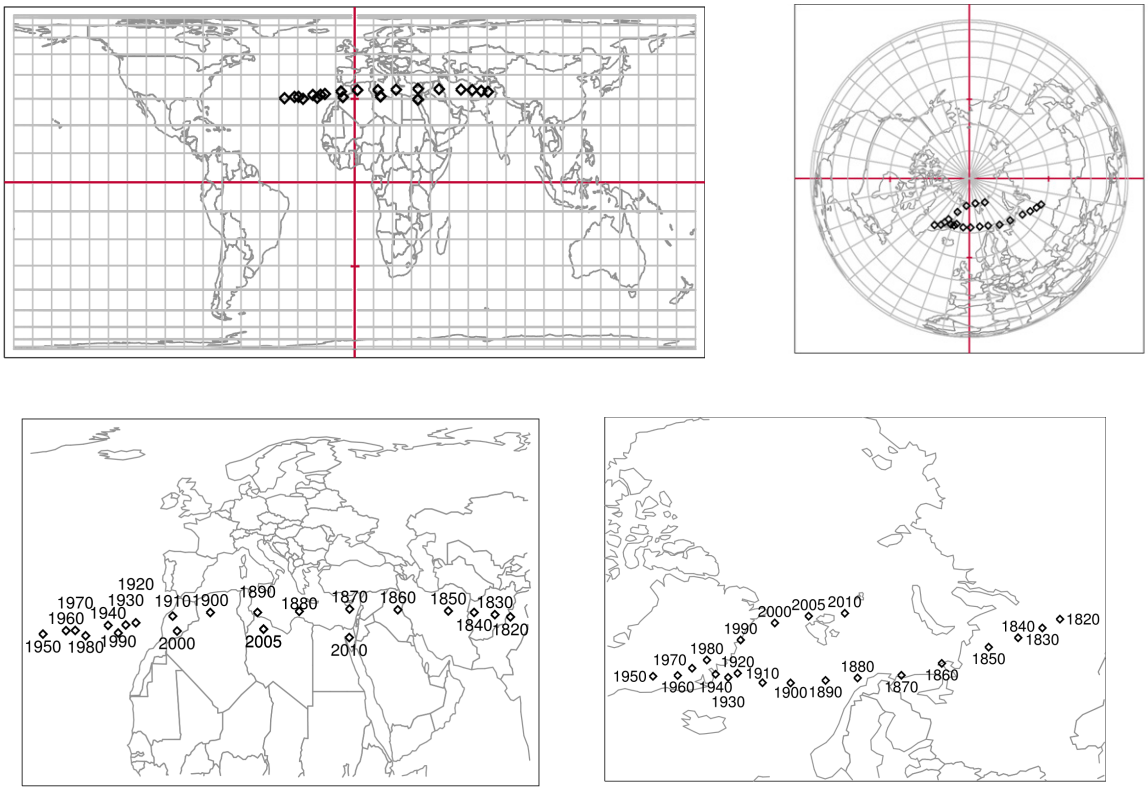

Figure 6: Center of gravity for GDP

Since 1950, the eastward shift has been steady, driven by European reconstruction first, and then by the Asian comeback. It seems to accelerate a lot between 2000 and 2010, when the center

of gravity jumps by more than 40° of longitude. However, while interpreting left maps, one has to remember that longitudes are not a precise concept in terms of distances. It does not only depend on latitude (which is here roughly constant), but also on the distance from the North-South axis, i.e. the inward location of the gravity center within the sphere, which is indicated on the right map. And, precisely between 2000 and 2010, it happens that the center of gravity gets quite close to the Earth center, ending a continuous decrease in the length of the vector since 1950. As a result, the effective speed in 2010 remains smaller than in 1950 that is, it is indeed large but not extraordinarily so. This explains the apparent jump and illustrates again how relying on a unique map to represent a three dimensional movement is misleading.

4.3. CO_2 emissions

The trajectory of the center of gravity for emissions is even more remarkable than for GDP. It is initially an almost purely British phenomenon, with a center of gravity locating just underneath the UK, with a length corresponding to 98% of the Earth's ratio. As the industrial revolution spreads, and the use of coal as the main energy source with it, this center begins its descent towards the South-West and the Earth's center. Its most westward location is in 1920, when its projection gets close to the US coast and its length has decreased to 81% of the Earth's ratio. During that first period, the speed is similar to the one recorded for the economic center of gravity, although larger for the last two decades of the sub-period (1910 and 1920). Overall, the 19th century is a period during which GDP and CO_2 emissions tend to evolve synchronically and westward. This is due to the progressive replacement of the UK by the US as the major source of world emissions. US dominance peaks in 1920, with a share of 50% of world emissions.

Comparative dynamics of GDP and emissions are altered after World War I. While economic expansion pursues its westward trend, the center of gravity of CO_2 emissions shifts towards the East in 1930 and 1940. This suggests a decoupling between economic activity and pollution, which is probably linked with the early adoption of oil as an alternative, less emission-intensive, source of energy by the US (i.e. the major polluter), while other major polluters remain more coal-dependent. Indeed, according to Smil (2010), the share of coal in US energy supply peaks in 1910, while it does so only 40 years later in the UK and the USSR. As a result, the share of the US in world emissions declines strongly in 1930-1940, whereas its GDP share remains stable. This explains the earlier reversal of the emission center of gravity with respect to the economic one. Economic trends remain powerful however, and the US growth spurt following the end of World War II temporarily interrupts the eastern trend in 1950, when both centers of gravity shift westward again, albeit more modestly for the emission center.

From 1950 onward, the emission center of gravity is heading East, as the economic one. This is in line with a decline in US dominance in terms of both GDP and emissions, although the decline is a lot larger for emissions, with a US share in world emissions dropping from above 40% in 1950 to 20% in 1980. This coincides with very large distances covered by the emission center of gravity, close to 1000 km per decade, as reported by figure 8. This suggests again that the transition towards non-coal energy sources such as oil and gas has been quicker in the US compared to other large emitters (the share of coal falls below 50% as early as 1940 for the US, but only in 1960 for the UK or Japan, and 1970 for Russia, see Smil (2010).

During the first two decades following the end of the cold war, 1990 and 2000, the eastern shift is slowed down, as the US share in world totals either stabilizes for emissions or even increases slightly

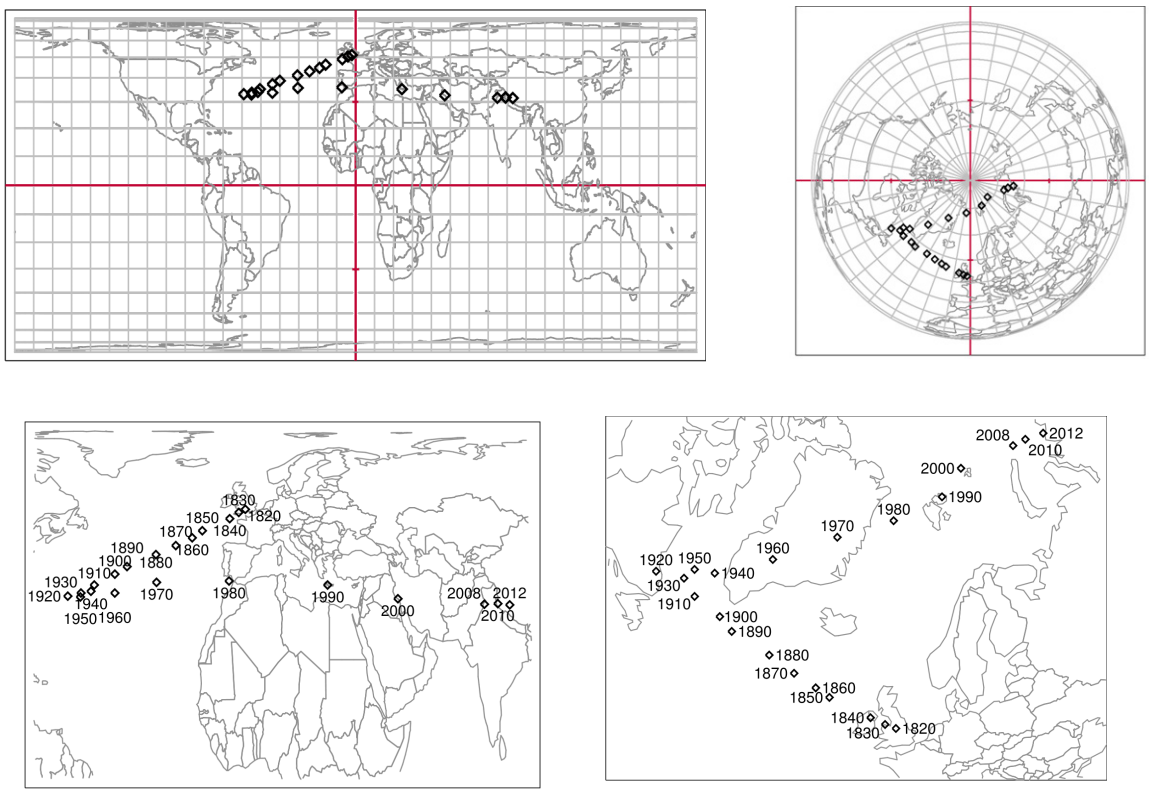

Figure 7: Center of gravity for CO_2 emissions

for GDP. This is in line with a pause in the erosion of US dominance and the demise of the USSR.[7] But the movement accelerates again in the last decade, 2010, for both GDP and emissions. This corresponds to the rise of Asian countries, in particular China, which remains heavily dependent on coal as an energy source. By the end of the sample period, the emission center of gravity locates quite close to the demographic center of gravity.

In a nutshell, the evolution of the emission center of gravity suggests radical changes in the spatial distribution of CO_2 emissions on the Earth's surface. In two centuries, it shifts from an extremely concentrated location to one which is strikingly similar to the distribution of world population. This calls for a complementary analysis in the last subsection.

[7]We warn again the reader against using the left map only to estimate distances covered by the emission center of gravity in 1990 and 2000. They appear large, in particular in contrast with 1960. However, as shown by the right map, it is a typical "wiper" effect due to the fact that the center of gravity locates closer and closer to the Earth's center from 1950 onward. In reality distances covered are considerably smaller in 1990 or 2000 than in 1960 (see figure 8).

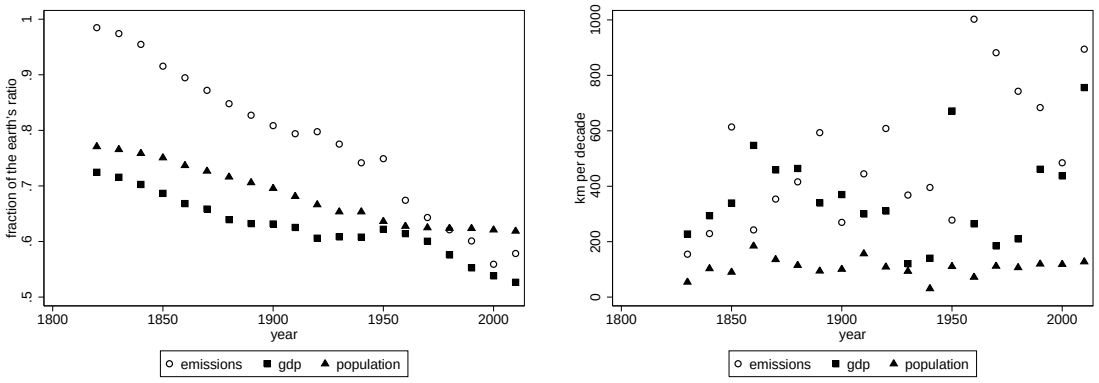

(a) (b)

Figure 8: Length and speed for the centers of gravity

5. Spatial imbalances: measurement and discussion

People are unequally spread across the planet's surface, i.e. mainly in the Northern Hemisphere, and mostly in Asia. This encapsulates into a location of the demographic center of gravity which is roughly stable over time, at 0.5R (R=6371km) above the equatorial plane and 0.5R to the right of the Greenwich meridian. If GDP and emissions were equally shared among people, the corresponding centers of gravity would locate at the same place, i.e. below Northern India, at roughly 70% from the center of the Earth. This is not what happened during the last two centuries. From there the idea of using the distance between the demographic center of gravity and the comparison one as a proxy for the spatial imbalances characterizing the per capita distribution of the underlying variable (either GDP or emissions).

More specifically, following Zhao et al. (2003), we define the index of spatial imbalances as the ratio between the actual distance between the demographic center of gravity and the one it is compared to, and the potential maximum for that distance, i.e. the length of the demographic center of gravity vector plus the Earth's radius.[8] Applied to GDP and emissions, this leads to the values reported in Figure 9.

What happens for GDP confirms the trend reversal pattern already identified in figure 6. Spatial imbalances start below 10%, and then increase during the Big Divergence, as economic growth takes off in Western countries and their offshoots. The peak is reached in 1950, with an index slightly over 50%. After that, European and then most importantly Asian catch-up decrease spatial imbalances back to 20% at the end of the period.

[8] For example, if the demographic center of gravity is denoted by D, the economic center of gravity by G, and the Earth's center by O, then the index of spatial imbalances for GDP is given by $\frac{\left\|\overrightarrow{DG}\right\|}{\left[\left\|\overrightarrow{DO}\right\|+R\right]}$, where R is the Earth's radius.

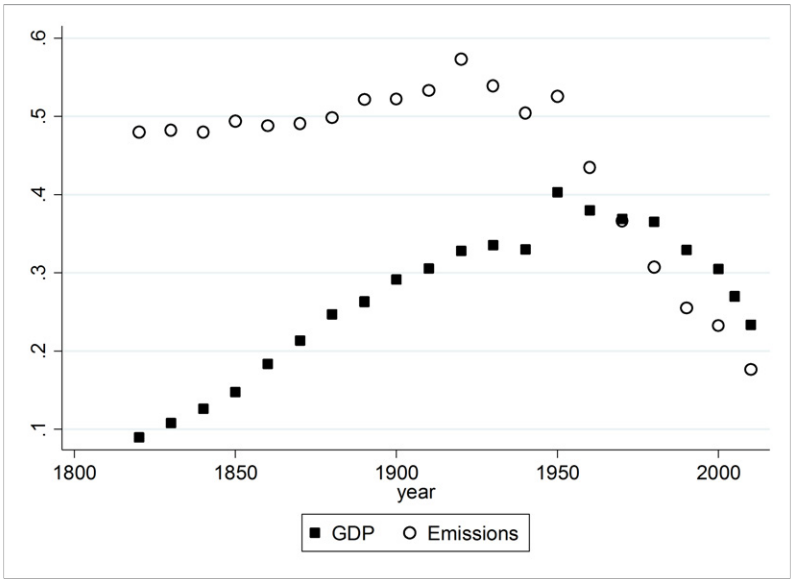

Figure 9: Indices of spatial imbalances

The temporal pattern for emissions is distinct in that it starts from a large level of close to 50% in 1820. The rest of the trajectory is qualitatively similar to GDP, i.e. also an inverted-u shape, but with three differences. First, the rising phase is less steep, with a peak at 60%. This is due to the fact that, apart from going West, which increases the index, the center of gravity of emissions is also going down (Southward), which decreases the index. Second, as already noticed in figure 7, the peak is reached in 1920, not 1950. Third, the decreasing phase is steeper, with a final index of spatial imbalances for emissions around 10% in 2010.

Intuitively, if data had been available for earlier centuries, it is quite probable that the pattern of spatial imbalances for emissions would have looked even more similar to the one for GDP. After all, before any country started its industrial revolution, differences in emissions per capita across countries were probably not large, implying a low level of spatial imbalances. This suggests a kind of leading role of emissions with respect to GDP over a long time span.

Although no formal analysis has been performed, the interpretation would be as follows. Start from a pre-industrial world where production and emissions are roughly homogeneous across people. Then technological innovation and the use of fossil fuels give an early boost to Western countries. The impact on emissions is immediate, while the effect on production takes several decades to materialize. During the rest of the 19th century and the early 20th century, as the West industrializes alone, emissions and production go hand in hand. Then the rapid adoption of less emission-intensive energy sources (oil and gas rather than coal) by the US sends back the emission center of gravity towards the East as early as the 1930s. Economic activity is characterized by more inertia, but when it starts to shift back as well after 1950, this accelerates further the eastern movement in emissions, also enhanced by the shift of more emission-intensive manufacturing activities towards

Asia. As it happens, after a long period of divergence, both the economic and the emission centers of gravity seem to be dragged back to their initial 1820 location determined by demography.[9]

The above trends are confirmed when using alternative conventions regarding the smoothing shift from CDIAC to EDGAR data for emissions, or from Maddison to GEcon data for GDP. Moreover, temporal patterns for the demographic and economic centers of gravity are similar to those identified by **?**, even though they did not rely on the Hyde database to capture within-country changes in spatial distributions. Therefore, given data limitations, our results can be considered as reasonably robust.

6. Conclusions

During the two centuries that followed the industrial revolution, economic activity has become more intense, complex and widespread upon the Earth's surface. This has coincided with a redistribution of people, power and pollution across regions. Capturing the major trends underpinning these spatial changes is not straightforward. By synthesizing the spatial distribution of any variable into a single point, the world center of gravity approach allows to reveal interesting dynamics. We have applied that approach to three variables i.e. human population, GDP and CO_2 emissions, for which gridded data were made available along the 1820-2010 period. We have also refined the presentation of results in order to avoid distortions and identify more accurately critical reversals.

Two major results emerge. First, the world demographic center of gravity is very stable over time, and clearly located under Asia. Second, the other two variables present a strong divergence with respect to demography during the 19th century, and a progressive return towards Asia during the 20th century, with a reversal in 1920 for emissions, and 1950 for GDP. Technological innovation, energy transition, structural change and wars are the main factors underlying these trends and turning points. In a nutshell, it is as if demography acts like a long run anchor, while emissions and GDP are two outcome variables of a technological diffusion process which increases spatial inequalities during the 19th century and progressively decreases them during the 20th century.

Two caveats to conclude. First, results could be refined with better quality data, in particular for the years before 1950. Second, and perhaps more fundamentally, this type of analysis may be discarded as being merely descriptive. We perfectly acknowledge that it is not a causal analysis. However, we believe it clarifies the presentation of trends and the identification of turning points that matter at the global level. As such, it may be applied to the many other cases where the relevant question is how do socio-economic phenomena spread across the Earth's surface.

[9]The extreme spatial concentration of emissions at the beginning of the sample period is due to the narrow definition of CDIAC historical data, limited to fossil fuel consumption and cement production only. However, to our knowledge, it is the best historical data on CO_2 emissions available at present.

Appendix A

Figure A1 reports, for each variable of interest, the evolution of the share of the largest six countries in world totals over the sample period.

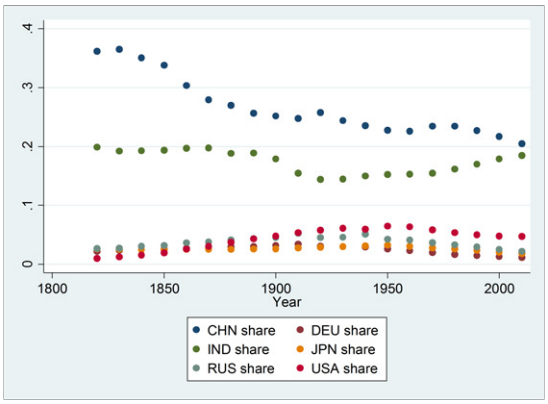

(a) Population

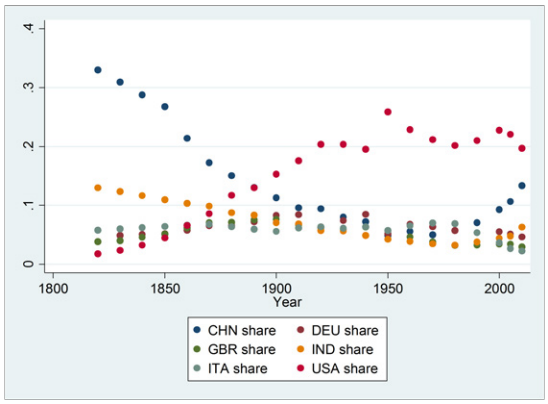

(b) GDP

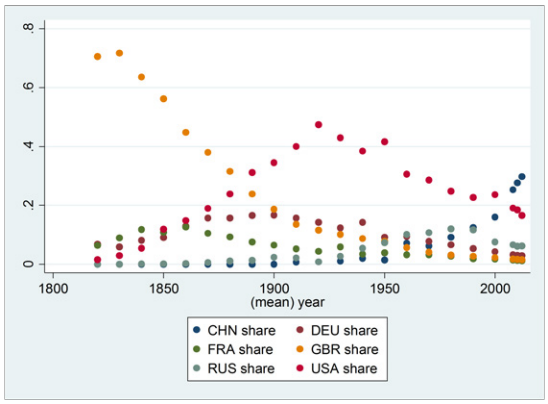

(c) CO_2 emissions

Figure A1: Shares of major countries in world totals 1820-2010

Acknowledgements

We thank Jim de Melo and Marcelo Olarreaga for very helpful comments, and the Swiss National Science Foundation for financial support under project 138625. The usual disclaimers apply.

7. References

Bairoch, P., 1971. Le Tiers-Monde dans l'impasse. Le démarrage économique du XVIIIe au XXe si ècle. Gallimard, Paris.

Barrett, S., Stavins, R., December 2003. Increasing Participation and Compliance in International Climate Change Agreements. International Environmental Agreements: Politics, Law and Economics 3 (4), 349–376.

Boden, T., Marland, G., Andres, R., 2013. Global, regional and national fossil-fuel co2 emissions. Tech. rep., Carbon Dioxide Informaton Analysis Center, Oak Ridge National Laboratory, U.S. Departement of Energy, Oak Ridge, Tenn. U.S.A.

Ellis, E. C., Kaplan, J. O., Fuller, D. Q., Vavrus, S., Goldewijk, K. K., Verburg, P. H., 2013. Used planet: A global history. Proceedings of the National Academy of Sciences 110 (20), 7978–7985.

European Commission, Joint Research Centre (JRC)/Netherlands Environmental Assessment Agency (PBL), 2011. Emission database for global antrospheric research (EDGAR), release version 4.2.
URL `http://edgar.jrc.ec.europa.eu`

G-Econ, 2011. Geographically based economic data.
URL `http://gecon.yale.edu`

GADM, 2012. GADM database of global administrative areas, version 2.0.
URL `www.gadm.org`

Grether, J.-M., Mathys, N. A., 2010. Is the world's economic centre of gravity already in asia? Area 42 (1), 47–50.

Grether, J.-M., Mathys, N. A., 2011. Frontiers of Economics and Globalization, Vol 11: Economic Growth and Development. Emerald Group, London, Ch. On the Track of the World's Economic Center of Gravity, pp. 261–287.

Klein Goldewijk, K., Beusen, A., van Drecht, G., de Vos, M., 2011. The hyde 3.1 spatially explicit database of human-induced global land-use change over the past 12,000 years. Global Ecology and Biogeography 20 (1), 73–86.

Maddison, A., 2010. Statistics on world population, gdp and per capita gdp.
URL `http://ggdc.net/MADDISON/`

Matthews, H. D., Graham, T. L., Keverian, S., Lamontagne, C., Seto, D., Smith, T. J., 2014. National contributions to observed global warming. Environmental Research Letters 9 (1), 014010.

Mattoo, A., Subramanian, A., 2012. Equity in Climate Change: An Analytical Review. World Development 40 (6), 1083–1097.

Nordhaus, W., Azam, Q., Corderi, D., Hood, K., Makarova, N., Mohammed, M., Miltner, A., Weiss, J., 2006. The G-Econ database on gridded output: methods and data.
URL `http://gecon.yale.edu`

Quah, D., 2011. The global economy's shifting center of gravity. Global Policy 2 (1), 3–9.

Smil, V., 2010. Energy Transition: History, Requirements, Prospects. Praeger, Santa Barbara, CA.

Snyder, J., 1987. Map Projections: A Working Manual. No. 1395 in US Geological Survey Professional Paper. US Government Printing Office, Washington.

The Maddison Project, 2013. 2013 version.
URL http://www.ggdc.net/maddison/maddison-project/home.htm

Zhao, Z., Stough, R. R., Li, N., 2003. Note on the measurement of spatial imbalance. Geographical Analysis 35 (2), 170–176.